



This discussion paper is/has been under review for the journal Geoscientific Model Development (GMD). Please refer to the corresponding final paper in GMD if available.

Modelling turbulent vertical mixing sensitivity using a 1-D version of NEMO

G. Reffray¹, R. Bourdalle-Badie¹, and C. Calone²

¹Mercator Océan, Toulouse, France

²LGGE, Grenoble, France

Received: 2 July 2014 – Accepted: 15 July 2014 – Published: 8 August 2014

Correspondence to: G. Reffray (reffray@mercator-ocean.fr)

Published by Copernicus Publications on behalf of the European Geosciences Union.

GMDD

7, 5249–5293, 2014

Modelling turbulent vertical mixing sensitivity using a 1-D version of NEMO

G. Reffray et al.

Title Page

Abstract

Introduction

Conclusions

References

Tables

Figures

⏪

⏩

◀

▶

Back

Close

Full Screen / Esc

Printer-friendly Version

Interactive Discussion



Abstract

Through two numerical experiments, a 1-D vertical model called NEMO1D was used to investigate physical and numerical turbulent-mixing behaviour. The results show that all the turbulent closures tested ($k + l$ from Blanke and Delecluse, 1993 and two equation models: Generic Length Scale closures from Umlauf and Burchard, 2003) are able to correctly reproduce the classical test of Kato and Phillips (1969) under favourable numerical conditions while some solutions may diverge depending on the degradation of the spatial and time discretization. The performances of turbulence models were then compared with data measured over a one-year period (mid-2010 to mid-2011) at the PAPA station, located in the North Pacific Ocean. The modelled temperature and salinity were in good agreement with the observations, with a maximum temperature error between -2 and 2°C during the stratified period (June to October). However the results also depend on the numerical conditions. The vertical RMSE varied, for different turbulent closures, from 0.1 to 0.3°C during the stratified period and from 0.03 to 0.15°C during the homogeneous period. This 1-D configuration at the PAPA station (called PAPA1D) is now available in NEMO as a reference configuration including the input files and atmospheric forcing set described in this paper. Thus, all the results described can be recovered by downloading and launching PAPA1D. The configuration is described on the NEMO site (http://www.nemo-ocean.eu/Using-NEMO/Configurations/C1D_PAPA). This package is a good starting point for further investigation of vertical processes.

1 Introduction

Copernicus is a multidisciplinary programme of the European Union for sustainable services providing information on monitoring of the atmosphere, climate change, land and marine environments. The services also address the management of emergency and security-related situations (<http://www.copernicus.eu/>). The GMES (Global Monitoring

GMDD

7, 5249–5293, 2014

Modelling turbulent vertical mixing sensitivity using a 1-D version of NEMO

G. Refray et al.

Title Page

Abstract

Introduction

Conclusions

References

Tables

Figures

⏪

⏩

◀

▶

Back

Close

Full Screen / Esc

Printer-friendly Version

Interactive Discussion



Modelling turbulent vertical mixing sensitivity using a 1-D version of NEMO

G. Refray et al.

[Title Page](#)

[Abstract](#)

[Introduction](#)

[Conclusions](#)

[References](#)

[Tables](#)

[Figures](#)

[⏪](#)

[⏩](#)

[◀](#)

[▶](#)

[Back](#)

[Close](#)

[Full Screen / Esc](#)

[Printer-friendly Version](#)

[Interactive Discussion](#)

for Environment and Security) marine service was the precursor of Copernicus and has ensured the systematic monitoring and forecasting of the state of oceans at regional and global scales. Within the GMES/MyOcean project, Mercator Océan, one of the French operational oceanography teams has implemented an operational, global, eddy-resolving system at $1/12^\circ$ and a regional system at $1/36^\circ$ covering the French and Iberian Peninsula coasts. The NEMO (Nucleus for European Modelling of the Ocean, Madec, 2008) ocean model has been used for both systems.

NEMO is a numerical-modelling tool developed and operated within a European consortium. Its code enables investigation of oceanic circulation (OPA) and its interactions with the atmosphere. Ice models (LIM) and biogeochemical models (TOP – PISCES or LOBSTER) could also be coupled. This primitive equation model offers a wide range of applications from short term forecasts (Mercator-Ocean and MyOcean/Copernicus), climate projections (Voltaire et al., 2013) to process studies (for example Chanut et al., 2008; Bernie et al., 2007).

OPA, the oceanic component of NEMO is built from the Navier–Stokes equations applied to the Earth referential system, in which the ocean is subjected to the Coriolis force. The prognostic variables are the horizontal components of velocity, the sea surface height and two active tracers (temperature and salinity).

These equations allow description of a wide range of processes at any spatial and temporal scales. This involves interpreting complex numerical results which means that it is difficult to improve the model due to the multiple non-linear interactions between the different equation terms. Fortunately, there are a lot of numerical test cases in the literature which make it possible to isolate each term of the equations (advection, diffusion or coordinate systems) and improve it independently of the others.

Vertical mixing plays an essential role in ocean dynamics and it must therefore be correctly estimated. In particular, it creates the mixed layer, the homogeneous ocean layer that interacts directly with the atmosphere, which can then be modelled as the Mixed Layer Depth (hereafter referred to as MLD). The MLD plays a very important role in the energetic exchanges between the ocean and the atmosphere and may have very

Modelling turbulent vertical mixing sensitivity using a 1-D version of NEMO

G. Refray et al.

[Title Page](#)

[Abstract](#)

[Introduction](#)

[Conclusions](#)

[References](#)

[Tables](#)

[Figures](#)

[⏪](#)

[⏩](#)

[◀](#)

[▶](#)

[Back](#)

[Close](#)

[Full Screen / Esc](#)

[Printer-friendly Version](#)

[Interactive Discussion](#)

high spatiotemporal variations (diurnal, seasonal, synoptical). In addition, MLD variability also plays a crucial role in biogeochemical processes. The deepening episodes of the MLD during winter inject nutrients into the euphotic layer with a strong impact on primary production (Flierl and Davis, 1993). Vertical mixing is also responsible for convection or seasonal stratification. Lastly, vertical mixing must be able to conserve the water masses.

To focus on vertical turbulent mixing, we use NEMO1D, a feature included in NEMO, to consider only one column of water. NEMO1D is a simple, robust, useful and powerful tool which enables quick and easy investigation of the physical processes affecting the vertical component of the ocean state variables: turbulence, surface and bottom boundary conditions, penetration radiation schemes, etc.

In this paper based on the 1-D configuration, we assess the effectiveness of different turbulent schemes available in NEMO. Section 2 describes how the turbulent closure was done. The numerical contexts (vertical grids and time steps) are listed in Sect. 3. Section 4 contains a discussion of how the turbulence models performed in relation to the empirical law which states that the mixed layer deepens as a function of time, as described by Kato and Phillips (1969) and based on a laboratory experiment. The sensitivity of the spatial and time discretization of each turbulent scheme is also discussed. Section 5 reports on of some experiments performed under realistic conditions and these turbulent closures are compared with data measurements taken at the PAPA station (<http://www.pmel.noaa.gov/OCS/Papa/index-Papa.shtml>). This buoy, located in a region of weak horizontal advection, is commonly used by the community to validate turbulent closures (Burchard et al., 2001). The last section contains the conclusion and perspectives for future investigation.

2 The NEMO 1-D framework

2.1 1-D simplification in the primitive equations

NEMO is based on the 3-D primitive equations but it offers the possibility of reducing the complexity of the system by limiting the domain to just one water column. This is the 1-D approach (hereafter called NEMO1D). It leads to the simplification of all horizontal gradients in the primitive equations.

The equation system then reduces to:

$$\frac{\partial u_i}{\partial t} = -\frac{\partial}{\partial z} \nu_t \frac{\partial u_i}{\partial z} + f_i \quad (1a)$$

$$\frac{\partial T}{\partial t} = \frac{1}{\rho_0 C_p} \frac{\partial I(F_{\text{sol}}, z)}{\partial z} - \frac{\partial}{\partial z} K_t \frac{\partial T}{\partial z} \quad (1b)$$

$$\frac{\partial S}{\partial t} = -\frac{\partial}{\partial z} K_t \frac{\partial S}{\partial z} + E_f - P_f \quad (1c)$$

where $u_{i\{i=1,2\}}$ represents the horizontal components of the velocity, T the temperature, S the salinity, $f_{i\{i=1,2\}}$ the components of the Coriolis term. I the downward irradiance, F_{sol} the penetrative part of the surface heat flux, ρ_0 the reference density and C_p the specific heat capacity. E_f and P_f are respectively the evaporation and precipitation fluxes while ν_t and K_t are respectively the turbulent viscosity and turbulent diffusivity. Lastly, z and t correspond respectively to the vertical and temporal dimensions.

The C-grid (Arakawa and Lamb, 1977) is commonly used in NEMO. For purely numerical reasons, the A-grid is henceforth used by NEMO1D as the velocity components and the scalar values are calculated at the same point.

Due to the equation simplifications and the low computational cost, NEMO1D is a perfect tool for studying the vertical component of NEMO.

GMDD

7, 5249–5293, 2014

Modelling turbulent vertical mixing sensitivity using a 1-D version of NEMO

G. Refray et al.

Title Page

Abstract

Introduction

Conclusions

References

Tables

Figures

◀

▶

◀

▶

Back

Close

Full Screen / Esc

Printer-friendly Version

Interactive Discussion

2.2 Vertical turbulence models

The turbulence issue raises the question of how to compute accurately the coefficients ν_t and K_t in Eqs. (1a)–(1c). There are many ways of computing these turbulent coefficients. The simplest method involves replacing them by constant values or parameterizing them as a function of the Richardson number Ri defined as the ratio of the buoyancy to the shear:

$$\nu_t = \frac{\nu_{t0}}{(1 + a Ri)^b} \quad (2a)$$

$$K_t = \frac{K_{t0}}{(1 + a' Ri)^{b'}} \quad (2b)$$

$$Ri = \frac{N^2}{M^2} \text{ with } N^2 = -\frac{g}{\rho_0} \frac{\partial \rho}{\partial z} \text{ and } M^2 = \sum_{i=1}^2 \left(\frac{\partial u_i}{\partial z} \right)^2 \quad (2c)$$

where N^2 is the Brunt–Väisälä frequency, ρ the density and $g = 9.81 \text{ m s}^{-2}$ the gravitational acceleration. ν_{t0} and K_{t0} correspond to background values and a , b , a' and b' are constants depending on the selected closure (Munk and Anderson, 1948; Paconowski and Philander, 1981).

Other more complex methods require one or two supplementary differential equations. In these cases, the vertical turbulent viscosity ν_t and diffusivity K_t can be expressed as:

$$\nu_t = C_\mu \sqrt{k} l \quad (3a)$$

$$K_t = C'_\mu \sqrt{k} l \quad (3b)$$

where C_μ and C'_μ can represent stability functions or constants, k is the turbulent kinetic energy and l is the mixing length.

The problem is then reduced to determining the values of k , l , C_μ and C'_μ . The different ways of estimating these quantities are described in the following sections.

2.2.1 Turbulent kinetic energy

Turbulent kinetic energy (k) is computed according to the following transport equation:

$$\frac{\partial k}{\partial t} = D_k + P + G - \varepsilon \quad (4)$$

5 where D_k represents the turbulent and viscous transport terms expressed as:

$$D_k = \frac{\partial}{\partial z} \frac{\nu_t}{\sigma_k} \frac{\partial k}{\partial z} \quad (5)$$

with σ_k a constant Schmidt-number.

10 P and G in Eq. (4) relate to the production of turbulent kinetic energy respectively by shear and buoyancy:

$$P = \nu_t M^2 \quad (6a)$$

$$G = K_t N^2 \quad (6b)$$

15 However, G is a term for production of turbulent kinetic energy only in unstable situations. In stable situations, this term reflects the destruction of the turbulence due to stratification.

Finally, ε in Eq. (4) is the rate of dissipation:

$$\varepsilon = \left(C_\mu^0\right)^3 \frac{k^{3/2}}{l} \quad (7)$$

20 where C_μ^0 denotes a constant of the model.

2.2.2 The mixing length

There are two ways of computing a mixing length. First, it can be parameterized as suggested, for example, in Gaspar et al. (1990) or Xing and Davies (1999). This kind

of model can be regrouped in the $k + l$ family. Blanke and Delecluse (1993) have suggested estimating the mixing length as a ratio between the turbulent velocity fluctuations and the Brunt–Väisälä frequency:

$$l = \frac{2k^{1/2}}{N} \quad (8)$$

This relation is a simplification of the formulation of Gaspar et al. (1990). This model is the most frequently used by the NEMO community for turbulence closure, commonly called the TKE model.

The second way of computing a mixing length is to use an additional differential equation. The three models, mostly used by the ocean modelling community and based on a differential equation to determine the mixing length are: k - k/l (Mellor and Yamada, 1982), k - ε (Rodi, 1987) and k - ω (Wilcox, 1988). According to Umlauf and Burchard (2003), the turbulent quantities k , l , ε and ω can be expressed using a Generic Length Scale (hereafter referred to as GLS):

$$\Psi = (C_\mu^0)^p k^m l^n \quad (9)$$

where p , m and n are real numbers (see Table 1).

The transport equation for the variable Ψ can be formulated as:

$$\frac{\partial \Psi}{\partial t} = D_\Psi + \frac{\Psi}{k} (C_{\Psi 1} P + C_{\Psi 3} G - C_{\Psi 2} \varepsilon) \quad (10)$$

where $C_{\Psi 1}$, $C_{\Psi 2}$ and $C_{\Psi 3}$ are constants to be defined and D_Ψ represents the turbulent and viscous terms of Ψ expressed as:

$$D_\Psi = \frac{\partial}{\partial z} \frac{u_t}{\sigma_\Psi} \frac{\partial \Psi}{\partial z} \quad (11)$$

with σ_Ψ a constant Schmidt-number.

GMDD

7, 5249–5293, 2014

Modelling turbulent vertical mixing sensitivity using a 1-D version of NEMO

G. Refray et al.

Title Page

Abstract

Introduction

Conclusions

References

Tables

Figures

◀

▶

◀

▶

Back

Close

Full Screen / Esc

Printer-friendly Version

Interactive Discussion



Modelling turbulent vertical mixing sensitivity using a 1-D version of NEMO

G. Refray et al.

Title Page

Abstract

Introduction

Conclusions

References

Tables

Figures

⏪

⏩

◀

▶

Back

Close

Full Screen / Esc

Printer-friendly Version

Interactive Discussion



Thus, each turbulence model is defined by the following set of parameters: ρ , m , n , C_{μ}^0 , σ_{κ} , σ_{ψ} , $C_{\psi 1}$, $C_{\psi 2}$ and $C_{\psi 3}$ (see Table 1). Due to the main turbulence requirements (logarithmic boundary layer, mixed layer deepening or shear-free turbulence occurring in presence of surface wave breaking), an optimal set of these parameters has been suggested by Umlauf and Burchard (2003). This fourth, second-order turbulence model is called the “generic model”.

The results obtained with these four closures (k - k_l , k - ε , k - ω , generic deduced from the GLS formulation) and TKE are presented in this paper.

2.2.3 Stability functions

The stability functions appearing in Eqs. (3a) and (3b) are derived from the Reynolds stress equations and depend on the shear and buoyancy numbers, called respectively α_M and α_N and expressed as:

$$\alpha_M = \frac{k^2}{\varepsilon^2} M^2 \text{ and } \alpha_N = \frac{k^2}{\varepsilon^2} N^2 \quad (12)$$

There are several articles on stability functions in the literature. The main functions commonly used by the community are Galperin (1988), Kantha and Clayson (1994), Hossain (1980) and Canuto A and B (Canuto et al., 2001). This study does not discuss any sensitivity tests for these functions. This has in fact been done by Burchard and Bolding (2001) who claim that better results are obtained with the Canuto A stability functions. Thus, they were naturally chosen for the study presented in this paper and

are expressed as:

$$C_{\mu} = \frac{0.1070 + 0.01741\alpha_N - 0.00012\alpha_M}{1 + 0.2555\alpha_N + 0.02872\alpha_M + 0.008677\alpha_N^2 + 0.005222\alpha_M\alpha_N - 0.0000337\alpha_M^2} \quad (13a)$$

$$C'_{\mu} = \frac{0.1120 + 0.004519\alpha_N + 0.00088\alpha_M}{1 + 0.2555\alpha_N + 0.02872\alpha_M + 0.008677\alpha_N^2 + 0.005222\alpha_M\alpha_N - 0.0000337\alpha_M^2} \quad (13b)$$

2.2.4 Model constants

The values of constants (see Table 1) depend on the selected closure model.

For GLS closures, the values of C_{ψ_3} , under stable conditions, monitor the mixed layer deepening: Umlauf et al. (2003) or the manual of the General Ocean Turbulence Model (<http://www.gotm.net>). Indeed, a Richardson number can be computed in a homogeneous stratified shear-flow in steady state. This number called Ri_{st} depends on the stability functions and on C_{ψ_3} . The values of C_{ψ_3} shown in Table 1 were computed with $Ri_{st} = 0.25$ using the Canuto A stability functions. The value of 0.25 was fixed by comparison with the measurements of the Kato–Phillips experiment (further discussed in a next section). Then, the value of C_{ψ_3} for $k-k_l$ model was adjusted to 2.62 by Burchar (2001a). This value is significantly higher than the initial value of 0.9 suggested by Mellor-Yamada (1982). Some values for the other stability functions can be found in Warner et al. (2004).

The well-known failure of $k-k_l$ to respect the law of the wall required the addition of a wall function F_{WALL} to the C_{ψ_2} constant. The wall function implemented in NEMO was initially suggested by Mellor and Yamada (1982).

Another important constant appearing in the Table 1 is Pr , the Prandtl number defined as a function of the Richardson number (only for TKE):

$$\begin{cases} Pr = \frac{0.2}{Ri} & \text{if } Ri \geq Ri_c \\ Pr = 1 & \text{otherwise} \end{cases} \quad (14)$$

with $Ri_c = 0.2$ being the critical Richardson number.

Concerning the GLS models using stability functions, Pr is determined as:

$$Pr = \mu_t / K_t = C_\mu / C'_\mu \quad (15)$$

For information, the Ri_c for the stability functions of Canuto A is 0.847.

To ensure a minimum of mixing processes, we applied some background values to the following turbulence quantities: $u_{t_bg} = 1.2 \times 10^{-4} \text{ m}^2 \text{ s}^{-1}$, $K_{t_bg} = 1.2 \times 10^{-5} \text{ m}^2 \text{ s}^{-1}$, $k_{bg} = 10^{-6} \text{ m}^2 \text{ s}^{-2}$, $\varepsilon_{bg} = 10^{-12} \text{ m}^2 \text{ s}^{-3}$.

The other constants in Table 1 are discussed in the next section devoted to the surface boundary condition.

2.2.5 Surface boundary condition

The ocean surface is subjected to atmospheric forcing and eventually surface wave breaking that could induce significant mixing.

In the absence of an explicit wave description, the surface turbulent quantities can be described as a logarithmic boundary layer with the following properties:

$$k = \lambda u_*^2 \text{ if } P = \varepsilon \quad (16a)$$

$$l = \kappa(z + z_0) \quad (16b)$$

$$D_k = -\frac{u_t}{\sigma_k} \frac{\partial k}{\partial z} = 0 \quad (16c)$$

Modelling turbulent vertical mixing sensitivity using a 1-D version of NEMO

G. Refray et al.

Title Page

Abstract

Introduction

Conclusions

References

Tables

Figures

⏪

⏩

◀

▶

Back

Close

Full Screen / Esc

Printer-friendly Version

Interactive Discussion



where z is the distance from the sea surface, z_0 is the surface roughness, u_* is the friction velocity and λ is a constant depending on the turbulence closure.

Inside this logarithmic boundary layer, the turbulent kinetic energy is constant and its flux is zero. The constant depends on the turbulence model and can be expressed as:

$$\lambda = \frac{1}{\sqrt{c_\mu (c_\mu^0)^3}} = 3.75 \text{ for TKE closures} \quad (17)$$

$$\lambda = \frac{1}{(c_\mu^0)^2} \sim \frac{1}{0.3} \sim 3.33 \text{ for GLS closures} \quad (18)$$

Both these values are closed to the typical value of $\frac{10}{3}$ given by Townsend (1976) for a logarithmic boundary layer.

If the surface breaking waves mixing is considered, then shear-free turbulence may be assumed. This special case is characterized by a spatial decay of turbulence away from a source without mean shear. In these conditions, the turbulence solution can be written as:

$$k = K(z + z_0)^\alpha \quad (19a)$$

$$l = L(z + z_0) \quad (19b)$$

$$D_k = \varepsilon \quad (19c)$$

where z_0 is expressed as a function of the wave age as suggested by Raschle et al. (2008):

$$z_0 = \frac{\text{Frac}_{\text{HS}}}{0.85} \frac{1}{665 \cdot g} u_*^2 W_{\text{age}}^{\frac{3}{2}} \text{ with } W_{\text{age}} = 30 \tanh\left(\frac{2 \cdot 0.3}{28 u_*}\right) \quad (20)$$

Modelling turbulent vertical mixing sensitivity using a 1-D version of NEMO

G. Reffray et al.

Title Page	
Abstract	Introduction
Conclusions	References
Tables	Figures
◀	▶
◀	▶
Back	Close
Full Screen / Esc	
Printer-friendly Version	
Interactive Discussion	



and α is the decay exponent for the turbulent kinetic energy expressed as:

$$\alpha = - \frac{4n(\sigma_k)^{1/2}}{(1+4m)(\sigma_k)^{1/2} - (\sigma_k + 24\sigma_k C_{\psi 2})^{1/2}} \quad (21)$$

and L is a constant of proportionality for the length scale expressed as:

$$L = C_{\mu}^0 \left(\frac{C_{\mu}^0}{C_{\mu}^{\text{sf}}} \right)^{1/2} \left(\frac{(1+4m+8m^2)\sigma_k + 12\sigma_{\psi} C_{\psi 2} - (1+4m)(\sigma_k(\sigma_k + 24\sigma_{\psi} C_{\psi 2}))^{1/2}}{12n^2} \right)^{1/2} \quad (22)$$

with C_{μ}^{sf} being the shear free value of the stability function estimated to 0.73 for the Canuto A. This value is slightly higher than the value of $C_{\mu}^0 = 0.5268$ established inside the logarithmic boundary layer.

For the GLS closures, the surface boundary condition for k is formulated under the flux form (Craig and Banner, 1996):

$$D_k = - \frac{u_t}{\sigma_k} \frac{\partial k}{\partial z} = C_w u_*^3 \left(\frac{z+z_0}{z_0} \right)^{3\alpha/2} \quad (23)$$

with C_w an empirical parameter depending on the wave age and usually estimated to be $C_w = 100$ for a fully developed wave or $C_w = 0$ if no surface wave breaking is considered to again fall within the Relation (16c).

Note that the value of α in Eq. (21) must be between -2 and -3 , and the value of L in Eq. (22) must be slightly inferior than the Von Karmann constant $\kappa = 0.41$. The values of α and L computed with the k - ε are not correct when the value of α is too high or

Modelling turbulent vertical mixing sensitivity using a 1-D version of NEMO

G. Refray et al.

Title Page

Abstract

Introduction

Conclusions

References

Tables

Figures

⏪

⏩

◀

▶

Back

Close

Full Screen / Esc

Printer-friendly Version

Interactive Discussion



the value for L too low (Burchard, 2001b). To overcome this failure, the Relation (21) is used to compute the optimal σ_k obtained with $\alpha = -1.5$. A transition function is then necessary for σ_k to tend toward this surface value.

For TKE, the Relation (19) has been modified to set a value for the turbulent kinetic energy at the surface as proposed by Mellor and Blumberg (2004):

$$k = \frac{1}{2}(15.8C_w)^{\frac{2}{3}}u_*^2 \sim 67.83u_*^2 \quad (24a)$$

$$l = \kappa z_0 = \kappa \beta \frac{u_*^2}{\rho_0 g} \sim 8.2u_*^2 \quad (24b)$$

with $\beta = 2 \times 10^5$ an empirical constant (Stacey, 1999). In addition, to enable the mixing induced by breaking waves to penetrate the water column, a percentage of the surface turbulent kinetic energy is injected below the surface. The total turbulent kinetic energy is then determined as follows:

$$k_{\text{tot}}(z) = k_{\text{eq}}(z) + \alpha_{\text{bc}}k_{\text{bc}}(z=0)e^{-\frac{z}{H_p}} \text{ for } z \neq 0 \quad (25)$$

where k_{eq} is the turbulent kinetic energy computed with Eq. (4), k_{bc} is the surface turbulent kinetic energy computed with Eq. (24a), α_{bc} is a percentage set to 5 % and H_p is the depth of penetration. In most cases, in realistic ocean simulations, H_p varies as a function of the latitude (0.5 m at the equator to a maximum of 30 m at the middle latitudes).

For all models, a background value of the surface roughness is set to the value $z_{0_bg} = 0.02$ m.

2.3 Interpretation of the test cases

It is obvious that the TKE and GLS closures are very different from a purely physical aspect but also in the way they are implemented. If we were to perform a relevant comparison of these turbulence models, we should, for example, use the same boundary

Modelling turbulent vertical mixing sensitivity using a 1-D version of NEMO

G. Refray et al.

Title Page

Abstract

Introduction

Conclusions

References

Tables

Figures

◀

▶

◀

▶

Back

Close

Full Screen / Esc

Printer-friendly Version

Interactive Discussion



conditions or the same stability functions. The problem then simply involves comparing a parameterization of the mixing length to that obtained with a differential equation.

The purpose of this paper is to provide feedback on different turbulent closures available in NEMO and to allow users to choose or tune the most appropriate one with respect to the application in question.

3 Space and time discretization

The choice of the vertical grid is crucial. A compromise should be found between the resolution needed for a good representation of the oceanic processes, and the computational cost, linked to the number of cells and the CFL criteria (Courant Friedrichs Levy, 1928) which induce the time step constraint.

Currently, for realistic applications using NEMO, there are two classes of vertical grids:

- low-resolution vertical grids with the thickness of first levels between 6 m and 10 m. The grid with 31 cells (Fig. 1), delivered in the standard ORCA2 configuration of NEMO and specially designed for climate applications (Dufresne et al., 2013), is a good example. This is the grid selected for this study and it will be referred to as L31.
- high-resolution grids that typically have a thickness of 1 m in the first levels. The grid with 75 vertical cells described in Fig. 1 and referred as L75, represents this second class of vertical grids in our study. This grid is used in the global $1/4^\circ$ and in the regional $1/12^\circ$ Mercator Océan reanalyses (Ferry et al., 2010, 2011) but also in projects such as DRAKKAR (DRAKKAR group, 2007) or decadal predictions in the GIEC framework (Voldoire et al., 2013).

The more interesting aspect, with respect to the test case results presented in the next sections, concerns the resolution of the first ten meters in which the MLD takes place.

Modelling turbulent vertical mixing sensitivity using a 1-D version of NEMO

G. Reffray et al.

Title Page

Abstract

Introduction

Conclusions

References

Tables

Figures

◀

▶

◀

▶

Back

Close

Full Screen / Esc

Printer-friendly Version

Interactive Discussion



We note that L75 has more levels than L31 in the first fifty meters: 18 to 5. The layer thicknesses are of the order of 1 m in L75 but 10 m for L31.

Several time steps are used in three-dimensional simulations and these are fixed according to the spatial resolutions and their associated CFL conditions.

NEMO1D has no restriction on the time step, as there is no vertical advection and hence no CFL condition. However, we have tested the sensitivity of each turbulence model to the following time steps: 360 s, 1200 s and 3600 s. These time steps correspond to those used in the global configurations at Mercator Océan and more generally in the community. So, we can easily regroup some pairs [vertical grid, time step] to retrieve some known configurations:

- [L75, 360 s]: Global configurations at $1/12^\circ$ (Deshayes et al., 2014; Treguier et al., 2014) used in Mercator Océan forecast system (Dréville et al., 2008; Domrowsky et al., 2009)
- [L75, 1200 s]: Global configurations at $1/4^\circ$ used in global Mercator Océan reanalysis (Ferry et al., 2011) and DRAKKAR project (Barnier et al., 2006)
- [L31, 3600 s]: Global configurations at 1° used for climatic studies (Hewitt et al., 2011)
- [L75, 3600 s]: Global configurations at 1° used for decadal forecast in the GIEC framework (Voltaire et al., 2013)

Special attention will be paid to these four pairs when we interpret the numerical results.

4 Idealized test case: the Kato–Phillips experiment

4.1 Description

The Kato–Phillips (1969) experiment is classically used in the literature to test and calibrate turbulence models (for example Burchard, 2001a; Galperin, 1988). This

Modelling turbulent vertical mixing sensitivity using a 1-D version of NEMO

G. Refray et al.

Title Page

Abstract

Introduction

Conclusions

References

Tables

Figures

◀

▶

◀

▶

Back

Close

Full Screen / Esc

Printer-friendly Version

Interactive Discussion



However, the numerical MLDs were slightly underestimated by approximately 1 m: the RMSEs were between 0.9 m for $k-\varepsilon$ and 1.4 m for TKE.

4.3 Results

In realistic 3-D global or regional configurations, the numerical framework is less favourable for obvious CPU time or storage reasons. The vertical grids are then coarser (typically L31 or L75) with greater time steps. Nevertheless, these time steps are limited by the CFL condition, mainly on the vertical, and thus set by the choice of the grid. This numerical restriction does not occur in NEMO1D due to the no-advection assumption. Consequently, we have taken into account the 60 possibilities (5 turbulence models \times 3 vertical grids \times 4 time steps). As stated previously, we focussed on the four pairs described at the end of Sect. 3. As expected, as shown in Fig. 3, the deepening of the MLDs cannot be continuous in time but occurs in steps, determined by the vertical resolution. The number of levels near the surface is crucial to this process.

For the pair [L75, 360 s] (Fig. 3a), all the models yielded suitable results with associated RMSEs of the order of 3 m. For the pair [L75, 1200 s] (Fig. 3b), all the models were close with RMSEs around 4 m, except for $k-\omega$ which exhibited a high RMSE value of 10 m. Concerning the pair [L75, 3600 s] (Fig. 3c), $k-\varepsilon$ and TKE exhibited the best results with a RMSE slightly greater than 7 m. The three others models did not provide satisfying results in this numerical context. The RMSEs were higher: 10, 13 and 15 m respectively for the generic, $k-k_l$ and $k-\omega$.

The numerical context of the pair [L31, 3600 s] (Fig. 3d) is obviously the most difficult. The L31 vertical grid is not well adapted for this test case due to its coarse surface layer resolution with a 10 m separation of the first levels. The thresholds linked to the vertical grid are such that the RMSE should not be compared to those obtained with the L75 grid. It should be noted in passing that (i) all closures represent the deepening of the maximum of N^2 (ii) all GLS closures show a quicker deepening of the MLD compared to the TKE solution. The MLD reaches 20 m during the first 10 h and there is no signal

Modelling turbulent vertical mixing sensitivity using a 1-D version of NEMO

G. Reffray et al.

Title Page

Abstract

Introduction

Conclusions

References

Tables

Figures

◀

▶

◀

▶

Back

Close

Full Screen / Esc

Printer-friendly Version

Interactive Discussion

with TKE closure. This is due to the implementation of the surface boundary condition on two points in the GLS closures.

To represent synthetically the 60 possibilities of our test cases, the performed statistics (RMSE and correlation) were condensed in a Taylor diagram (Fig. 4). Note that the red and blue cloud points, relative to the tests done respectively with L1000 and L75 grids, are, for most of them, statistically close to the reference solution with a standard deviation lower than 25 % and a correlation greater than 95 %. However, $k-\omega$ and $k-k'$ appear to be very sensitive to the chosen time step (number 3 and 4 in red and blue on the diagram) and have a normalized RMSE weaker than 0.75, even though the correlation is still good (greater than 0.95).

The green points relative to tests using the L31 grid, show that all the turbulence models yielded very similar results at this resolution. The dispersion was only due to the normalized standard deviation while the RMSEs are similar. This kind of scatter is only influenced by the fact that the solution could be above or below the step of the coarse vertical discretization near the surface (Fig. 3d).

5 PAPA station

5.1 Description

The PAPA station, located west of Canada, in the Pacific Ocean (50° N, 145° W) has been intensively studied in the literature (Gaspar, 1990; Burchard, 2001a; Mellor and Durbin, 1975). The resulting measurements are particularly well adapted for a study following a 1-D approach, and for validating and calibrating any turbulence model. Indeed, there is no interaction with the coast and the horizontal advections of heat and salt are weak. High quality measurements of ocean properties (temperature, salinity, velocities) and atmospheric conditions (wind, humidity, air temperature, heat fluxes and precipitation rate) are available for this site.

GMDD

7, 5249–5293, 2014

Modelling turbulent vertical mixing sensitivity using a 1-D version of NEMO

G. Refray et al.

Title Page

Abstract

Introduction

Conclusions

References

Tables

Figures

◀

▶

◀

▶

Back

Close

Full Screen / Esc

Printer-friendly Version

Interactive Discussion



Modelling turbulent vertical mixing sensitivity using a 1-D version of NEMO

G. Refray et al.

Title Page

Abstract

Introduction

Conclusions

References

Tables

Figures

◀

▶

◀

▶

Back

Close

Full Screen / Esc

Printer-friendly Version

Interactive Discussion

they are only available once a day. However, these data are useful for checking that the ECMWF atmospheric fields are relevant enough to be used with confidence. Statistical comparisons (mean of the model minus observations, correlation coefficients and root mean square errors) are shown in Table 2. Mean errors for wind velocities and air temperature are very small (respectively 1 m s^{-1} and $0.02 \text{ }^\circ\text{C}$) and the correlations are greater than 0.98. The atmospheric model assimilates these data. The radiative fluxes are well correlated contrary to the precipitation rate with a correlation coefficient of only 0.76. There is no marked seasonal cycle concerning the precipitation rate in observed data and ECMWF outputs (not shown in this paper). We conclude that the ocean summer stratification is primarily due to atmospheric heat fluxes. The relative humidity correlates well but shows a constant bias (RMSE value very close to the mean bias value) of almost 6%. Globally, these statistics show that the atmospheric fields from the ECMWF system can be used for this study.

Regarding initial conditions, it would be ideal to initialize the model with temperature and salinity measurements taken at the PAPA station on 15 June 2011. However, the data cover only the first 200 m for salinity and the first 300 m for temperature. Moreover, the salinity and temperature data are not collected on the same vertical grid: 24 levels for the temperature as opposed to 18 levels for the salinity. Thus, below a depth of 200 or 300 m, data from the WOD09 climatology (Levitus et al., 2013) were considered. Fortunately, there is a close match between the measurements and the climatology data below a depth of 150 m (Fig. 6).

5.2.2 Model settings

For simulations under realistic conditions, the turbulence models should take into consideration mixing caused by breaking waves. Thus, the surface boundary conditions are those described in Sect. 2.1 (Eqs. (19)–(23) for the GLS models and Eq. (24) for the TKE model). Moreover, the TKE model takes into account the injection of surface energy inside the water column as described in Eq. (25). This parameterization depends on the parameters α_{bc} and H_p . In order to estimate their impact on the MLD

dynamics, three cases are considered, corresponding to the three cases available in NEMO for this latitude: $\alpha_{bc} = 0$ (no_penetration), $H_p = 10$ m and $H_p = 30$ m. Thus, three distinct TKE models are defined: TKE_0m, TKE_10m and TKE_30m.

The bulk formulae used have been described in Large and Yeager (1994). The albedo coefficient is set to 6 %, the atmospheric pressure to 108 000 Pa and the air density to 1.22 kg m^{-3} . For this study, the ocean surface velocities are not taken into consideration in the stress computation.

For these experiments, the two vertical grids (L31 and L75) and the three different time steps (360 s, 1200 s, 3600 s) described in Sect. 3 have been taken into account. All possible pairs with all closures (4 issued from GLS formulation and 3 different TKEs) have been performed. This involved 42 simulations. The next section gives the results obtained with the pair with the highest resolution [L75, 360 s]. This pair is the selected setting for the standard configuration PAPA1D. The last section discusses the spatio-temporal sensitivity.

5.3 Results with the pair [L75, 360 s]

Figure 7 (respectively Fig. 8) represents the observed temperature (respectively the observed salinity) at the PAPA station and the biases (model minus observation) obtained with different closures.

During the year of simulation, the summer stratification is well represented with an increase of temperature of 6°C at a depth of 10 m between the initialization (15 June) and the maximum at the beginning of September. The halocline is close to 100 m in depth except between November to February where it is located at 80 m in depth. This depth variation is probably due to advective effects and the model cannot reproduce the process. Inside the MLD formed by the stratification, an increase of freshwater from August to November can be observed with a minimum of 32.4 PSU in October.

In order to focus on two major steps of the annual cycle, daily temperature profiles for 12 September 2010 (strong summer stratification) and 12 October 2010 (beginning

Modelling turbulent vertical mixing sensitivity using a 1-D version of NEMO

G. Refray et al.

Title Page

Abstract

Introduction

Conclusions

References

Tables

Figures

⏪

⏩

◀

▶

Back

Close

Full Screen / Esc

Printer-friendly Version

Interactive Discussion

of the homogenization) are shown in Fig. 9. Thus, we observed for only one month, an MLD deepening of 25 m between the observed temperature profiles (dark line).

In all simulations, this annual cycle is found and the general behaviour is the same, except for the simulation TKE_30m in which the differences between simulated temperature minus measurements exhibit, during summer, a vertical dipole, with a colder temperature than that observed, reaching -2°C , in the first 40 m and warmer ($+2^{\circ}\text{C}$) below 40 m. This dipole is indicative of excessive mixing and the lack of stratification as shown in Fig. 9. The vertical temperature gradient for the TKE_30m experiment (pink line) is smoother than the observed one (dark line). Consequently, a large amount of heat is introduced into the ocean and leads to a warming of 2°C in the 40–120 m layer especially during autumn and winter. As the thermocline is not present, the seasonal variability of the salinity cannot be investigated (Fig. 8). During winter (November to March), the excessive turbulent mixing partially destroys the halocline and the biases show the formation of a vertical dipole with water that is too salty ($+0.15\text{PSU}$) in the upper 80 m and too fresh below, with respect to the observation data. Consequently we can conclude that the mixing is too strong in the first hundred meters in this experiment.

The biases obtained for the experiments with the other turbulence models ($k-\varepsilon$, generic, $k-\omega$, $k-k_l$, TKE_10m and TKE_0m) do not exhibit an excessive mixing as for the TKE_30m experiment. On the contrary, the models tend to stratify too much during the summer as shown in Fig. 7, in which the temperatures of all these closures are too warm in the first 20 m ($+1^{\circ}\text{C}$ for generic, $k-\omega$, $k-k_l$, TKE_0m and $+0.5^{\circ}\text{C}$ for $k-\varepsilon$, TKE_10m) and too cold in the layer 20–80 m (-2°C for generic, $k-\omega$, $k-k_l$, TKE_0m and -1°C for $k-\varepsilon$, TKE_10m) with respect to the observation data.

As the precipitation rate has little influence on MLD dynamics (see Sect. 5.2.1), the salinity biases (Fig. 8) are directly linked to the MLD thickness by mixing and by evaporation. For the period from June to September, all the models exhibit the same weak salinity biases, as the MLD deepening is similar in each case. In October, for generic, $k-\omega$, $k-k_l$, TKE_0m and TKE_10m closure, significant biases appear at a depth of 40 m ($+0.1\text{PSU}$) and are trapped between 80 m and 100 m ($> 0.2\text{PSU}$) from December to

GMDD

7, 5249–5293, 2014

Modelling turbulent vertical mixing sensitivity using a 1-D version of NEMO

G. Refray et al.

Title Page

Abstract

Introduction

Conclusions

References

Tables

Figures

◀

▶

◀

▶

Back

Close

Full Screen / Esc

Printer-friendly Version

Interactive Discussion

Modelling turbulent vertical mixing sensitivity using a 1-D version of NEMO

G. Refray et al.

Title Page

Abstract

Introduction

Conclusions

References

Tables

Figures

⏪

⏩

◀

▶

Back

Close

Full Screen / Esc

Printer-friendly Version

Interactive Discussion

the end of the simulation. Consequently, these trapped saltier waters modify the halocline structure and are not mixed with the surface water. This induces a freshwater bias (-0.1 PSU) in the first 80 m during March to June. Such biases are not found in the results obtained with k - ε . The key process seems to occur in October when the atmospheric heat fluxes decrease and lead to the destruction of the stratification, thus generating a significant mixing. The temperature profiles of 12 October, plotted in Fig. 9, show that only k - ε is able to correctly reproduce the MLD deepening. The underlying saltier waters are then correctly injected into the MLD. Due to that, k - ε is the only closure which conserves the halocline intact and there is no fresh bias at the end of the simulation.

Regarding the sensitivity of the TKE model to the H_p parameter, H_p appears to be critical. The value of 30 m is too high, at least for the geographic location of the PAPA station, and does not reproduce summer stratification or conserve the deep halocline. On the other hand, in the case where no penetration is considered, the model tends to over-stratify and the MLD is not thick enough. As expected, an intermediate value of 10 m provides more satisfying results but the setting of H_p can be more complex in the case of global ocean simulations.

5.4 Spatiotemporal sensitivity

As in Sect. 4.3, this section covers the sensitivity of the different closures to the vertical discretization (grid L75 and L31) and to the time step (360 s, 1200 s and 3600 s). Figure 10 shows the evolution of the temperature RMSE for the different closures, computed for the first 120 m of the water column for the different closures (depth corresponding to the halocline depth, Fig. 5).

In all cases, two periods can be distinguished: (i) from June 2010 to November 2010 corresponding to the stratified period, for which high variations of the RMSE have been observed (between 0.03 to 0.35 °C) (ii) from December 2010 to June 2011, corresponding to the period when no stratification takes place, for which the RMSE of all

simulations is constant over the period (close to 0.12°C for TKE_30m and 0.05°C for other closures).

In both periods, the three TKE closures (red, orange and pink lines) do not show any significant sensitivity to the vertical discretization or the time step. This result is in agreement with the Kato–Phillips results presented in Sect. 4.

For the GLS closures, the two periods should be studied separately:

- During the first period (June 2010 to November 2010), the $k-\omega$ and $k-k_l$ show a high sensitivity to the time step for a high-resolution grid (L75) as expected according to the Kato–Phillips results (Sect. 4.3). For example, with the $k-\omega$ closure and the L75 grid the maximum of RMSE is 0.28°C with a time step of 360 s and increases to 0.35°C with a time step of 3600 s (green line on the Fig. 10). The time step variations have a weaker impact with L31 than with L75. The RMSE with $k-\omega$ stays close to 0.3°C in all L31 experiments. This result means that the time-step sensitivity is directly proportional to the vertical resolution. For a fixed grid, the generic and $k-\varepsilon$ closures do not show a high sensitivity to the time-step (dark and light blue in Fig. 10). The $k-\varepsilon$ closure gives the best results between these two closures exhibiting an RMSE ranging between 0.03°C and 0.2°C . The generic RMSE varies from 0.05°C to 0.25°C .
- During the second period (December 2010 to June 2011), all the RMSEs are similar and weak (0.05°C). The temporal variations over this period are small. Moreover, the closures have a small sensitivity to the vertical discretization and to the time step.

The RMSEs for $k-\varepsilon$ closure are better from August to September with L31 compared to those obtained with L75. For example, for 20 August and 360 s, the RMSE of the simulation with L75 is 0.15°C and decreases to 0.08°C with L31 (dark blue line in Fig. 10).

To focus on this point, vertical temperature profiles for both vertical grids were plotted for this date (Fig. 11). L75 tends to over-stratify and this result is in agreement with the

Modelling turbulent vertical mixing sensitivity using a 1-D version of NEMO

G. Refray et al.

Title Page

Abstract

Introduction

Conclusions

References

Tables

Figures

⏪

⏩

◀

▶

Back

Close

Full Screen / Esc

Printer-friendly Version

Interactive Discussion



previous section (Fig. 7). The profile obtained with L31 agrees better with the observations (dark line). This is due to the numerical dilution effect of the coarse grid in the surface layer. Indeed, this grid has only 3 levels in the first 30 m and is not able to create a strong stratification. In this case, a low vertical resolution becomes an advantage simply for numerical reasons.

6 Conclusions and perspectives

This paper has described the 1-D model version available in NEMO. This model is very useful for isolating and studying vertical processes, and for improving their representation before switching to a 3-D model.

The present study focused on the behaviour of turbulence closures available in NEMO, i.e. TKE and GLS. There are many differences between these two approaches, both with respect to the mixing length estimate and to the constants used or boundary conditions. For this reason, we did not concentrate on comparing the closures but rather their different strengths and weakness. Two test cases were selected, an “idealized” one, based on the experiment described in Kato–Phillips, and a “realistic” one, reproducing one year of salinity and temperature measured at the PAPA buoy.

The first test case was based on observations performed in laboratory. This experiment deals with the monitoring of the MLD deepening of an initially linear stratified fluid only subjected to a stationary surface stress. Because of its simplicity, this test case offers a perfect context for validating the numerical assumptions and implementations. Simulations were performed under favourable numerical conditions (grid with a resolution of 0.1 m and a time step of 36 s). All the turbulence closures correctly reproduced the experimental results described. This validates their implementation in NEMO. However, we found some dependence on numerical conditions (ratio time step/vertical discretization) for the GLS closures. This dependence is strong for $k-\omega$ and $k-k_l$ and a little smaller for generic and $k-\varepsilon$. The TKE closure does not show sensitivity to the numerical conditions but does underestimate the MLD.

Modelling turbulent vertical mixing sensitivity using a 1-D version of NEMO

G. Refray et al.

Title Page

Abstract

Introduction

Conclusions

References

Tables

Figures

⏪

⏩

◀

▶

Back

Close

Full Screen / Esc

Printer-friendly Version

Interactive Discussion



The data collected at the PAPA station are typically used to perform studies with 1-D models. This mooring was naturally chosen to create a new reference configuration for NEMO. This new configuration was described, and then used to complement our study of TKE and GLS closures. The results show that these closures are able to largely reproduce the stratification/homogenization cycle observed at the station.

We have also demonstrated the major impact of boundary conditions in TKE closure, via the parameter H_p that represents TKE penetration depth. Neglect of this TKE induces too strong a stratification and a value of 30 m, which is too high, thus inducing too much mixing inside the water column. The best results are obtained with an intermediate value of 10 m. The problem raised by this parameter estimation (spatiotemporal dependence), highlights the difficulty of tuning the TKE model in a realistic 3-D simulation. GLS closures gave correct results despite excessive summer stratification. Similar results to those of the Kato-Philipps experiment have been found for sensitivity to the numerical conditions (time step and vertical discretization): TKE closure has not shown any sensitivity, generic and $k-\varepsilon$ are slightly sensitive and $k-\omega$ and $k-k_l$ are very sensitive.

A key process has also been highlighted, namely the representation of salinity, occurring during the homogenization event in mid-October. All the models, except $k-\varepsilon$, underestimated the mixing and lead to significant salinity biases in the vicinity of the halocline. These biases persisted throughout the entire simulation. Nevertheless, we found no signature for the temperature field. The $k-\varepsilon$ closure correctly simulates the homogenization phase. This is the only closure which conserves the halocline and exhibits the weaker salinity biases.

The results obtained with NEMO1D were successfully compared with laboratory observations or in situ measurements through a turbulent closure sensitivity study. The 1-D approach, applied at the PAPA station (new NEMO reference configuration PAPA1D) or at another location, could be useful for further investigation of the turbulent mixing or some other physical component affecting vertical processes. Indeed, the MLD is

GMDD

7, 5249–5293, 2014

Modelling turbulent vertical mixing sensitivity using a 1-D version of NEMO

G. Refray et al.

[Title Page](#)

[Abstract](#)

[Introduction](#)

[Conclusions](#)

[References](#)

[Tables](#)

[Figures](#)

[⏪](#)

[⏩](#)

[◀](#)

[▶](#)

[Back](#)

[Close](#)

[Full Screen / Esc](#)

[Printer-friendly Version](#)

[Interactive Discussion](#)

subject to complex interactions between the turbulence, the surface forcing (including atmospheric fluxes and waves) and the boundary treatments.

Some of these following questions could be investigated using this numerical tool:

What is the behaviour of the other turbulence models of NEMO (KPP (Large et al., 1994) and Paconowski and Philander (1981)? What is the more adapted value of some parameters (H_p , surface roughness, background values . . .)? What is the sensitivity of the stability function? What would be the impact of another atmospheric dataset (observed data or coming from another meteorological centre) or the forcing frequency (one day, three hours, one hour, etc.)? What would be the impact of another forcing function (bulk formulae, flux form or atmospheric boundary layer model)? What would be the wave impact characterized for example through the Stokes drift or the Langmuir cells? What would be the impact of the solar flux penetration scheme that could incorporate two aspects: the chlorophyll fields used (temporal variability, observed at the surface or 3-D simulated field) or the penetration radiation schemes (Red-Green-Blue scheme such as the one used in this paper or Kpar formulation depending only on an attenuation depth)?

Finally, this 1-D model could also be useful for studies on coupling with atmospheric, ice or biogeochemical models.

Acknowledgements. This research was supported by the MyOcean2 European project and Mercator Océan. The authors wish to thank collaborators who have contributed to development of the NEMO ocean code as part of the NEMO consortium.

References

- Arakawa, A. and Lamb, V. R.: Computational design of the basic dynamical processes of the UCLA general circulation model, *Meth. Comp. Phys.*, 17, 173–265, 1977.
- Barnier, B., Madec, G., Penduff, T., Molines, J.-M., Treguier, A.-M., le Sommer, J., Beckmann, A., Biastoch, A., Böning, C., Dengg, J., Derval, C., Durand, E., Gulev, S., Remy, E., Talandier, C., Theetten, S., Maltrud, M., Mc Clean, J., and de Cuevas, B.: Impact of partial

GMDD

7, 5249–5293, 2014

Modelling turbulent vertical mixing sensitivity using a 1-D version of NEMO

G. Refray et al.

Title Page

Abstract

Introduction

Conclusions

References

Tables

Figures

◀

▶

◀

▶

Back

Close

Full Screen / Esc

Printer-friendly Version

Interactive Discussion

Modelling turbulent vertical mixing sensitivity using a 1-D version of NEMO

G. Refray et al.

Title Page

Abstract

Introduction

Conclusions

References

Tables

Figures

◀

▶

◀

▶

Back

Close

Full Screen / Esc

Printer-friendly Version

Interactive Discussion

- steps and momentum advection schemes in a global circulation model at eddy permitting resolution, *Ocean Dynam.*, 56, 543–567, doi:10.1007/s10236-006-0082-1, 2006.
- Bernie, D. J., Guilyardi, E., Madec, G., Slingo, J. M., and Woolnough, S. J.: Impact of resolving the diurnal cycle in an ocean-atmosphere GCM. Part 1: A diurnally forced OGCM, *Clim. Dynam.*, 29, 575, doi:10.1007/s00382-007-0249-6, 2007.
- 5 Blanke, B. and Delecluse, P.: Variability of the Tropical Atlantic Ocean simulated by a general circulation model with two different mixed-layer physics, *J. Phys. Oceanogr.*, 23, 1363–1388, 1993.
- Burchard, H.: On the $q2l$ equation by Mellor and Yamada (1982), *J. Phys. Oceanogr.*, 31, 1377–1387, 2001a.
- 10 Burchard, H.: Simulating the wave-enhanced layer under breaking surface waves with two-equation turbulence models, *J. Phys. Oceanogr.*, 31, 3133–3145, 2001b.
- Burchard, H. and Bolding K.: Comparative analysis of four second-moment turbulence closure models for the oceanic mixed layer, *J. Phys. Oceanogr.*, 31, 1943–1967, 2001.
- 15 Burchard, H. and Umlauf, L.: A generic length-scale equation for geophysical turbulence models, *J. Mar. Res.*, 61, 235–265, 2003.
- Canuto, V. M., Howard, A., Cheng, Y., and Dubovikov, M. S.: Ocean turbulence. Part I: One-point closure model-momentum and heat vertical diffusivities, *J. Phys. Oceanogr.*, 31, 1413–1426, 2001.
- 20 Chanut, J., Barnier, J., Large, W., Debreu, L., Penduff, T., Molines, J. M., and Mathiot, P.: Mesoscale eddies in the Labrador Sea and their contribution to convection and re-stratification, *J. Phys. Oceanogr.*, 38, 1617–1643, 2008.
- Courant, R., Friedrichs, K., and Lewy, H.: On the partial difference equations of mathematical physics, *IBM J. Res. Dev.*, 11, 215–234, 1928.
- 25 Craig, P. D. and Banner, M. L.: Modeling wave-enhanced turbulence in the ocean surface layer, *J. Phys. Oceanogr.*, 24, 2546–2559, 1994.
- Deshayes, J., Treguier, A., Barnier, B., Lecointre, A., Sommer, J. L., Molines, J.-M., Penduff, T., Bourdalle-Badie, R., Drillet, Y., Garric, G., Benschila, R., Madec, G., Biastoch, A., Boning, C., Scheinert, M., Coward, A. C., and Hirschi, J.: Oceanic hind-cast simulations at high resolution suggest that the Atlantic MOC is bistable, *Geophys. Res. Lett.*, 40, 3069–3073, 2013.
- 30 Dombrowsky, E., Bertino, L., Bassington, G. B., Chassignet, E. P., Davidson, F., Hurlburt, H. E., Kamachi, M., Lee, T., Martin, M. J., Mei, S., and Tonani, M.: GODAE systems in operation, *Oceanography*, 22, 80–95, 2009.

Modelling turbulent vertical mixing sensitivity using a 1-D version of NEMO

G. Reffray et al.

Title Page

Abstract

Introduction

Conclusions

References

Tables

Figures

◀

▶

◀

▶

Back

Close

Full Screen / Esc

Printer-friendly Version

Interactive Discussion

- Hewitt, H. T., Copsey, D., Culverwell, I. D., Harris, C. M., Hill, R. S. R., Keen, A. B., McLaren, A. J., and Hunke, E. C.: Design and implementation of the infrastructure of HadGEM3: the next-generation Met Office climate modelling system, *Geosci. Model Dev.*, 4, 223–253, doi:10.5194/gmd-4-223-2011, 2011.
- 5 Hossain, M. S.: *Mathematische Modellierung von turbulenten Auftriebsströmungen*, Ph.D. Dissertation, University of Karlsruhe, Germany, 145 pp., 1980.
- Jerlov, N. G.: *Optical Oceanography*, Elsevier, 194 pp., 1968.
- Kantha, L. H. and Clayson, C. A.: An improved mixed layer model for geophysical applications, *J. Geophys. Res.*, 99, 25235–25266, 1994.
- 10 Kato, H. and Phillips, O. M.: On the penetration of a turbulent layer into stratified fluid, *J. Fluid Mech.*, 37, 643–655, 1969.
- Large, W. G., McWilliams, J. C., and Doney, S. C.: Oceanic vertical mixing: a review and a model with a non-local boundary layer parameterization, *Rev. Geophys.*, 32, 363–403, 1994.
- Large, W. G. and Yeager, S. G.: Diurnal to decadal global forcing for ocean and sea-ice models: the data sets and flux climatologies, NCAR Technical Note, 1994.
- 15 Levitus, S., Antonov, J. I., Baranova, O. K., Boyer, T. P., Coleman, C. L., Garcia, H. E., Grodsky, A. I., Johnson, D. R., Locarnini, R. A., Mishonov, A. V., Reagan, J. R., Sazama, C. L., Seidov, D., Smolyar, I., Yarosh, E. S., and Zweng, M. M.: The World Ocean Database, *Data Science Journal*, 12, 229-234, Special Issue of the Proceedings of the 1st WDS Conference in Kyoto, 3–6 September 2011, Kyoto University, Kyoto, Japan, 2013.
- Madec, G.: *NEMO Reference Manual, Ocean Dynamics Component: NEMO-OPA*, Note du Pôle de Modélisation, 27, Institut Pierre-Simon Laplace (IPSL), France, 2008.
- McClain, C. R., Feldman, G. C., and Hooker, S. B.: An overview of the SeaWiFS project and strategies for producing a climate research quality global ocean bio-optical time series, *Deep-Sea Res. Pt. II*, 51, 5–42, 2004.
- 25 Mellor, G. and Blumberg, A.: Wave breaking and ocean surface layer thermal response, *J. Phys. Oceanogr.*, 34, 693–698, 2004.
- Mellor, G. and Durbin, P. A.: The structure and dynamics of the ocean surface mixed layer, *J. Phys. Oceanogr.*, 5, 718–728, 1975.
- 30 Mellor, G. and Yamada, T.: Development of a turbulence closure model for geophysical fluid problems, *Geop. and Space Physics*, 20, 851–855, 1982.
- Munk, W. H. and Anderson, E. R.: Notes on the theory of the thermocline, *J. Mar. Res.*, 3, 276–295, 1948.

Modelling turbulent vertical mixing sensitivity using a 1-D version of NEMO

G. Reffray et al.

Table 1. Turbulence model constants.

Constants	TKE	$k\text{-}k\text{l}$	$k\text{-}\varepsilon$	$k\text{-}\omega$	generic
p	–	0	3	–1	2
m	–	1	1.5	0.5	1
n	–	1	–1	–1	–0.67
C_μ	0.1	Canuto A	Canuto A	Canuto A	Canuto A
C_μ^r	0.1 Pr	Canuto A	Canuto A	Canuto A	Canuto A
$(C_\mu^0)^3$	0.7	$(0.5544)^3$	$(0.5477)^3$	$(0.5544)^3$	$(0.5544)^3$
C_{ψ_1}	–	0.9	1.44	0.555	1
C_{ψ_2}	–	0.5Fwall	1.92	0.833	1.22
C_{ψ_3} (stable)	–	2.62	–0.629	–0.64	0.05
C_{ψ_3} (unstable)	–	1	1	1	1
σ_κ	1	1.96	1	2	0.8
σ_ψ	–	1.96	1.2	2	1.07

Title Page

Abstract

Introduction

Conclusions

References

Tables

Figures

◀

▶

◀

▶

Back

Close

Full Screen / Esc

Printer-friendly Version

Interactive Discussion

Modelling turbulent vertical mixing sensitivity using a 1-D version of NEMO

G. Reffray et al.

Table 2. Comparisons of ECMWF atmospheric values and measurements at the PAPA station.

	T2m	Humidity	Wind <i>i</i>	Wind <i>j</i>	Solar flux	Non solar flux	Rain
Mean Bias (model minus observations)	0.02 °C	−6.13 %	0.54 m s ^{−1}	0.52 m s ^{−1}	10.3 W m ^{−2}	−11.64 W m ^{−2}	0.065 m d ^{−1}
Correlation	0.99	0.94	0.98	0.98	0.91	0.95	0.76
RMSE	0.33 °C	6.94 %	1.07 m s ^{−1}	1.26 m s ^{−1}	31.67 W m ^{−2}	16.5 W m ^{−2}	0.13 m d ^{−1}

Title Page

Abstract

Introduction

Conclusions

References

Tables

Figures

◀

▶

◀

▶

Back

Close

Full Screen / Esc

Printer-friendly Version

Interactive Discussion

Modelling turbulent vertical mixing sensitivity using a 1-D version of NEMO

G. Refray et al.

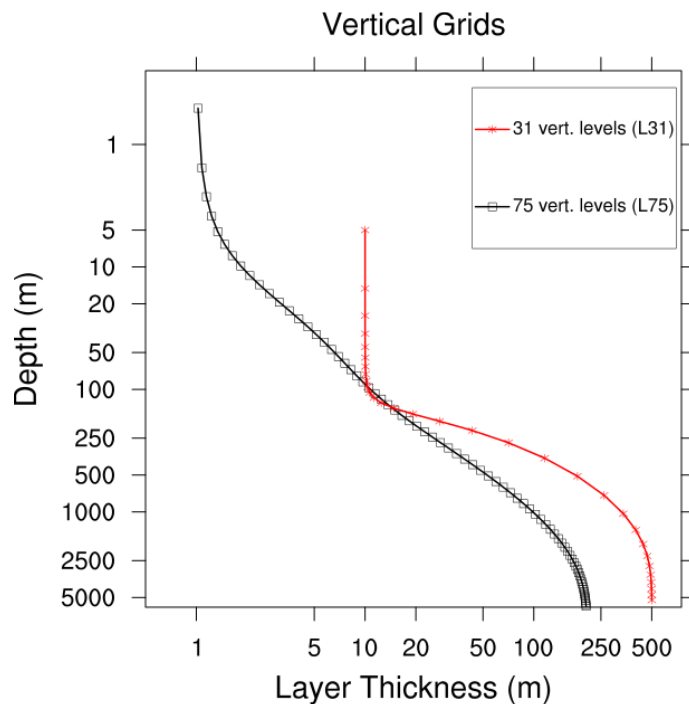


Figure 1. Thickness of vertical levels as a function of depth for two vertical grids: L31 (red) and L75 (black). Each plotting point (squares and stars) corresponds to the depth of levels.

[Title Page](#)[Abstract](#)[Introduction](#)[Conclusions](#)[References](#)[Tables](#)[Figures](#)[◀](#)[▶](#)[◀](#)[▶](#)[Back](#)[Close](#)[Full Screen / Esc](#)[Printer-friendly Version](#)[Interactive Discussion](#)

Modelling turbulent vertical mixing sensitivity using a 1-D version of NEMO

G. Refray et al.

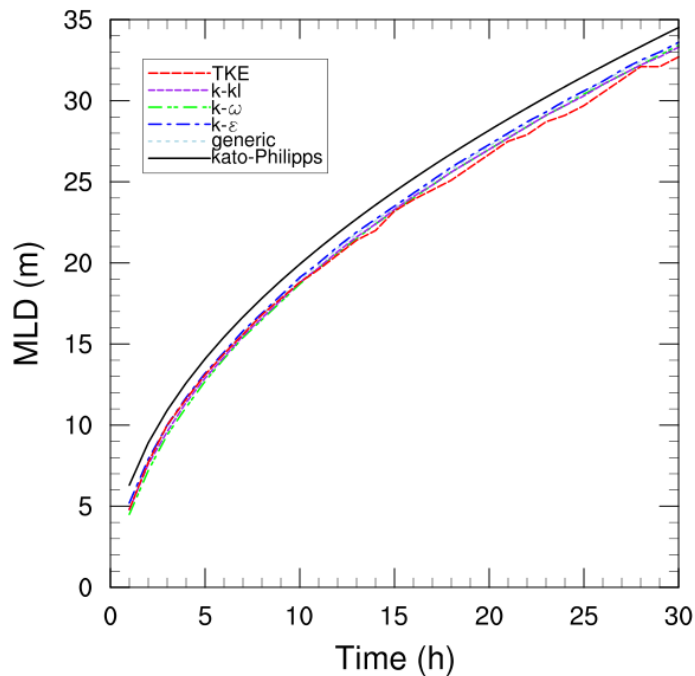


Figure 2. Time evolution of the MLD obtained as a function of the different turbulent closures with the 1000 levels vertical grid and a time step of 36 s. Analytic values are in black; generic in light blue; k - ϵ in dark blue, k - ω in green; k - kl in purple; and tke in red.

[Title Page](#)[Abstract](#)[Introduction](#)[Conclusions](#)[References](#)[Tables](#)[Figures](#)[◀](#)[▶](#)[◀](#)[▶](#)[Back](#)[Close](#)[Full Screen / Esc](#)[Printer-friendly Version](#)[Interactive Discussion](#)

Modelling turbulent vertical mixing sensitivity using a 1-D version of NEMO

G. Refray et al.

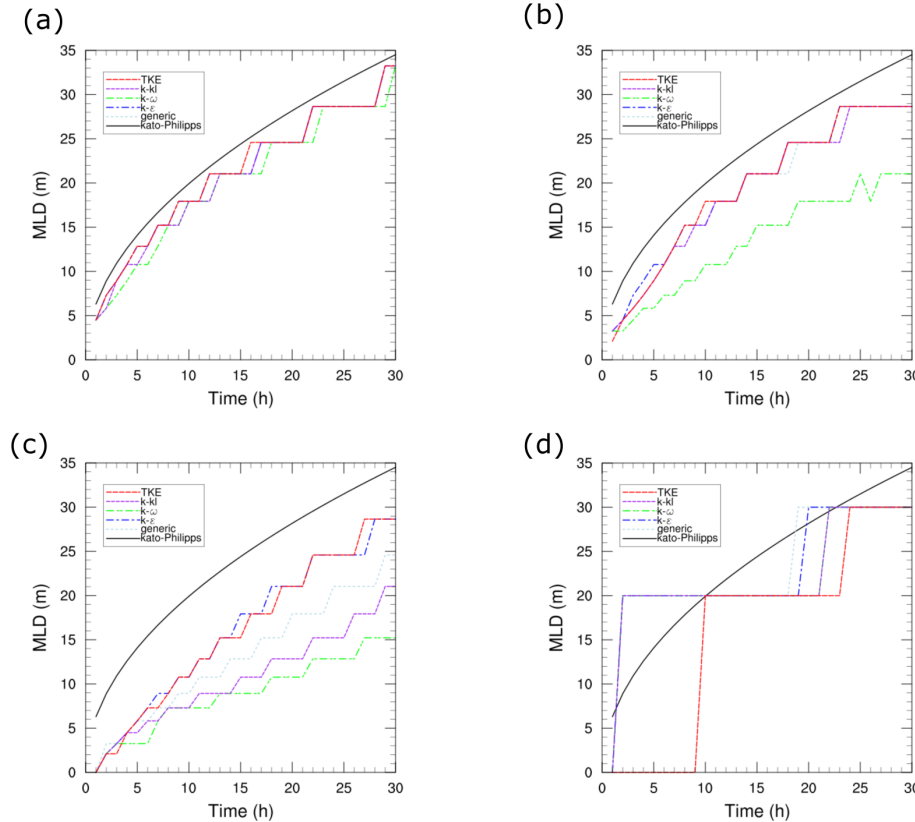


Figure 3. Time evolution of the MLD obtained with the different turbulence models for the pairs [L75, 360 s] **(a)**, [L75, 1200 s] **(b)**, [L75, 3600 s] **(c)**, [L31, 3600 s] **(d)**. Analytic values are in black; generic in light blue; $k-\epsilon$ in dark blue, $k-\omega$ in green; $k-k|$ in purple; and tke in red.

Title Page	
Abstract	Introduction
Conclusions	References
Tables	Figures
◀	▶
◀	▶
Back	Close
Full Screen / Esc	
Printer-friendly Version	
Interactive Discussion	



Modelling turbulent vertical mixing sensitivity using a 1-D version of NEMO

G. Reffray et al.

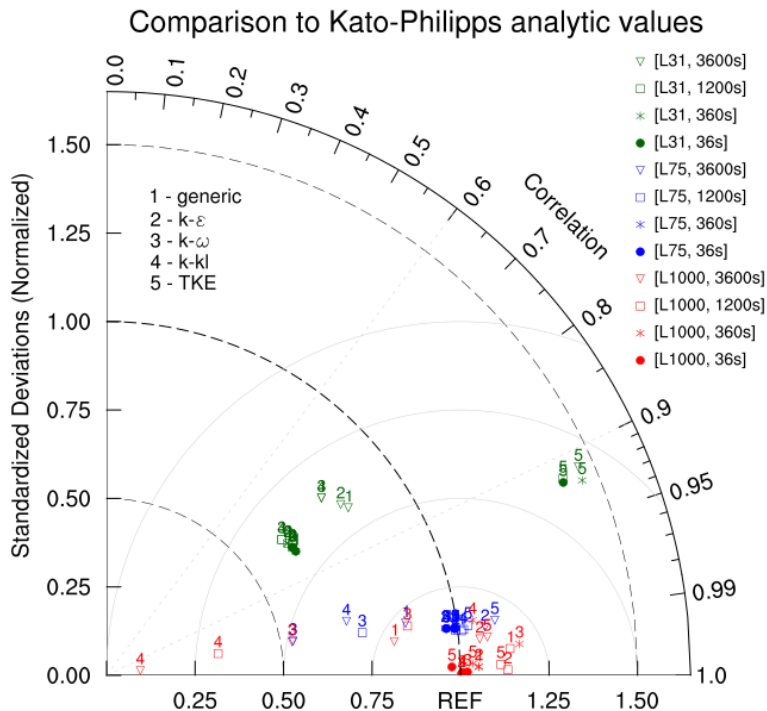


Figure 4. Taylor diagram of the 60 Kato–Phillips experiments. The number represents the closure (1 generic; 2 $k-\epsilon$; 3 $k-\omega$; 4 $k-k_l$; 5 tke); the colour represents the vertical grid (1000 levels in red; 75 levels in blue; 31 levels in green) and the form represents the time step (triangle 3600 s; square 1200 s; cross 360 s; point 36 s).

Title Page

Abstract

Introduction

Conclusions

References

Tables

Figures

◀

▶

◀

▶

Back

Close

Full Screen / Esc

Printer-friendly Version

Interactive Discussion



Modelling turbulent vertical mixing sensitivity using a 1-D version of NEMO

G. Refray et al.

Title Page

Abstract

Introduction

Conclusions

References

Tables

Figures

◀

▶

◀

▶

Back

Close

Full Screen / Esc

Printer-friendly Version

Interactive Discussion

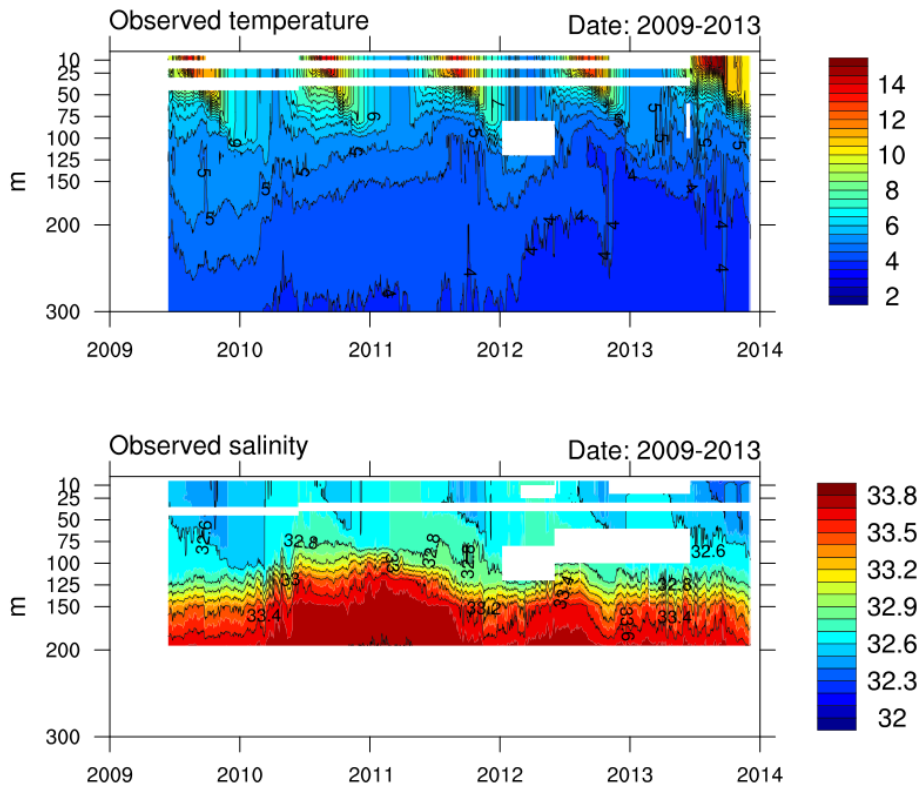


Figure 5. Temperature (top) and salinity (bottom) measured at the PAPA station covering the period 2009–2013.

Modelling turbulent vertical mixing sensitivity using a 1-D version of NEMO

G. Refray et al.

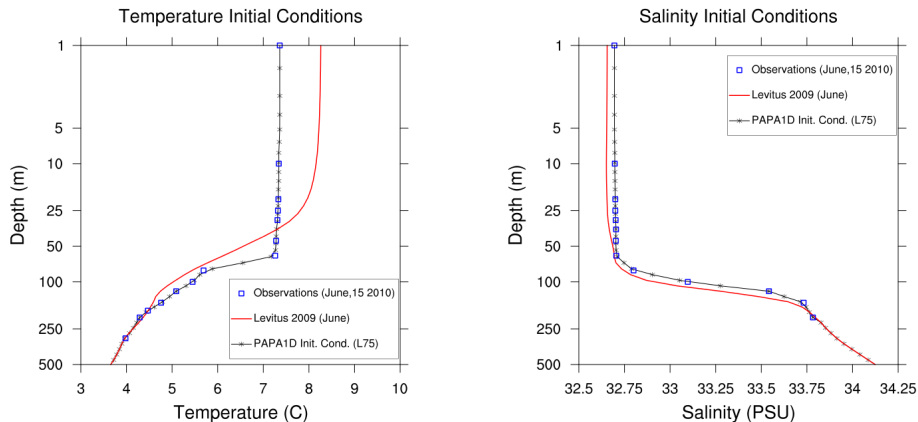


Figure 6. Initial conditions (black line and star) of temperature (left) and salinity (right) from measurements at the PAPA station (blue square) on 15 June 2010 and Levitus 2009 climatology data below (red).

[Title Page](#)[Abstract](#)[Introduction](#)[Conclusions](#)[References](#)[Tables](#)[Figures](#)[⏪](#)[⏩](#)[◀](#)[▶](#)[Back](#)[Close](#)[Full Screen / Esc](#)[Printer-friendly Version](#)[Interactive Discussion](#)

Modelling turbulent vertical mixing sensitivity using a 1-D version of NEMO

G. Refray et al.

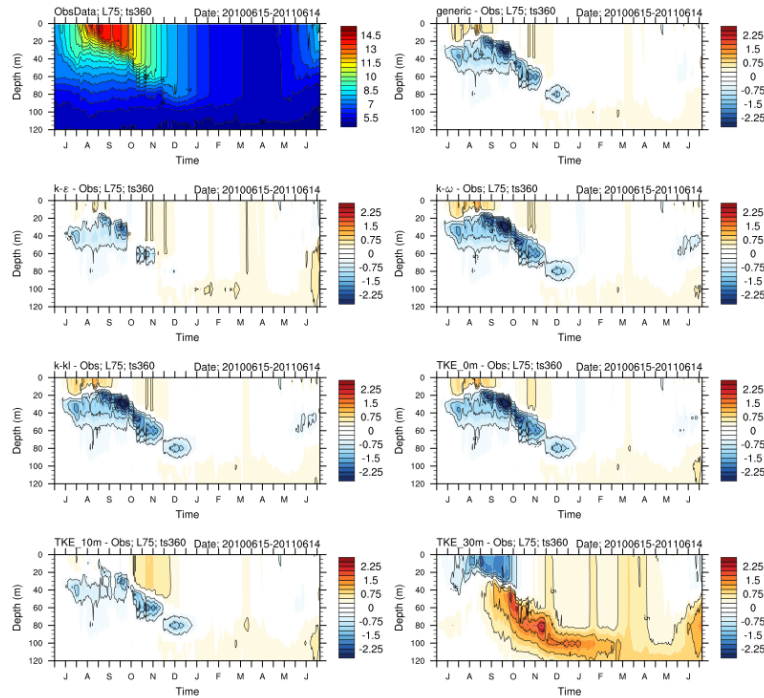


Figure 7. Observed temperature at PAPA station (top left) over the study period (15 June_2010 to 14 June 2011) and the biases (model minus observed data) obtained in the simulations with all closures, with [L75; 360 s]: generic (top right), $k-\varepsilon$ (middle high left), $k-\omega$ (middle high right), $k-k/l$ (middle bottom left), TKE_0m (middle bottom right), TKE_10m (bottom left) and TKE_30m (bottom right). Iso-lines are plotted every $0.5\text{ }^{\circ}\text{C}$ (except for the iso-0 which has not been plotted).

Title Page

Abstract

Introduction

Conclusions

References

Tables

Figures

◀

▶

◀

▶

Back

Close

Full Screen / Esc

Printer-friendly Version

Interactive Discussion

Modelling turbulent vertical mixing sensitivity using a 1-D version of NEMO

G. Refray et al.

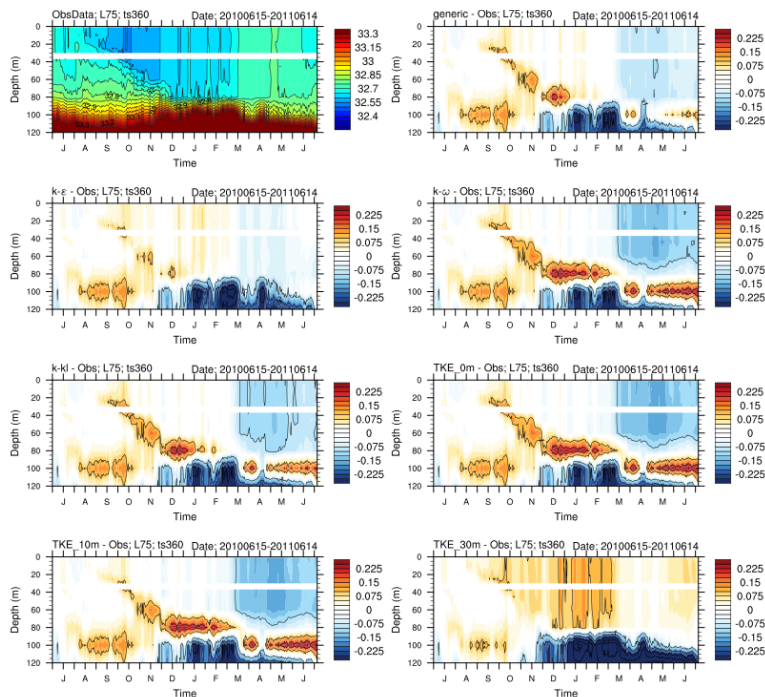


Figure 8. Observed salinity at PAPA station (top left) over the study period (15 June 2010 to 14 June 2011) and the biases (model minus observed data) obtained in the simulations with all closures, with [L75; 360 s]: generic (top right), k - ε (middle high left), k - ω (middle high right), k - k/l (middle bottom left), TKE_0m (middle bottom right), TKE_10m (bottom left) and TKE_30m (bottom right). Iso-lines are plotted every 0.1 PSU (except the iso-0 which has not been plotted).

Title Page

Abstract

Introduction

Conclusions

References

Tables

Figures

◀

▶

◀

▶

Back

Close

Full Screen / Esc

Printer-friendly Version

Interactive Discussion

Modelling turbulent vertical mixing sensitivity using a 1-D version of NEMO

G. Refray et al.

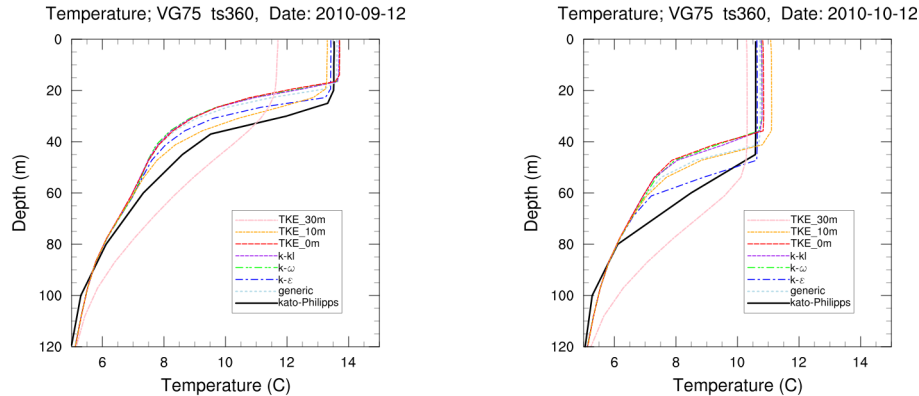


Figure 9. Daily vertical profiles of temperature during the stratified period (12 September 2010) on the left and at the beginning of the delayering period (12 October 2010) on the right. Observed data are in black, TKE_30m in pink, TKE_10m in orange, TKE_0m in yellow, $k-k_l$ in purple, $k-\omega$ in green, $k-\epsilon$ in dark blue and generic in light blue.

Title Page	
Abstract	Introduction
Conclusions	References
Tables	Figures
◀	▶
◀	▶
Back	Close
Full Screen / Esc	
Printer-friendly Version	
Interactive Discussion	

Modelling turbulent vertical mixing sensitivity using a 1-D version of NEMO

G. Refray et al.

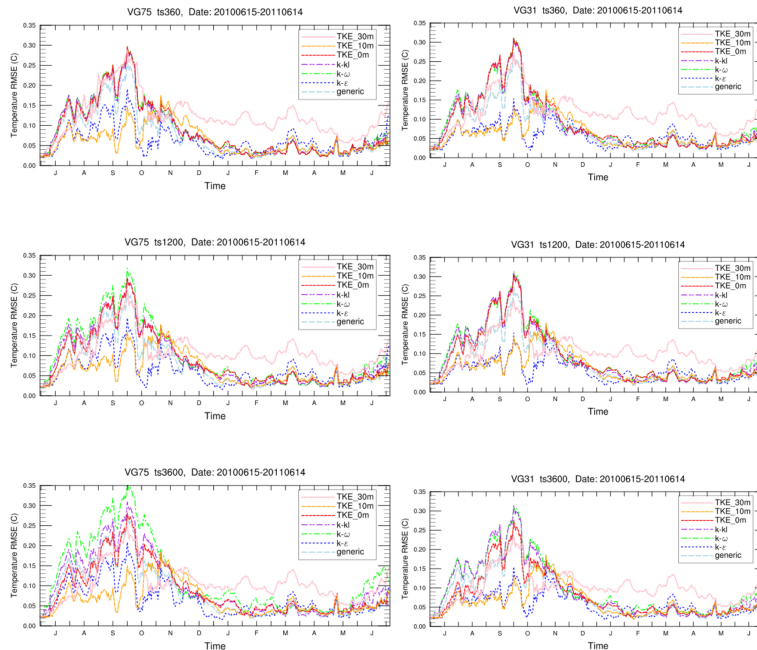


Figure 10. Evolution of the temperature RMSE computed along the vertical (0–120 m) for the different grids (L75 left column and L31 right column), different time steps (top panels 360 s, middle panel 1200 s, 3600 s bottom panels) and different closures (TKE_30m in pink, TKE_10m in orange, TKE_0m in yellow, $k-kI$ in purple, $k-\omega$ in green, $k-\epsilon$ in dark blue and generic in light blue).

Title Page	
Abstract	Introduction
Conclusions	References
Tables	Figures
◀	▶
◀	▶
Back	Close
Full Screen / Esc	
Printer-friendly Version	
Interactive Discussion	



Modelling turbulent vertical mixing sensitivity using a 1-D version of NEMO

G. Refray et al.

Title Page

Abstract

Introduction

Conclusions

References

Tables

Figures

◀

▶

◀

▶

Back

Close

Full Screen / Esc

Printer-friendly Version

Interactive Discussion

Temperature; VGL75 & VGL31 ts3600, Date: 2010-08-20

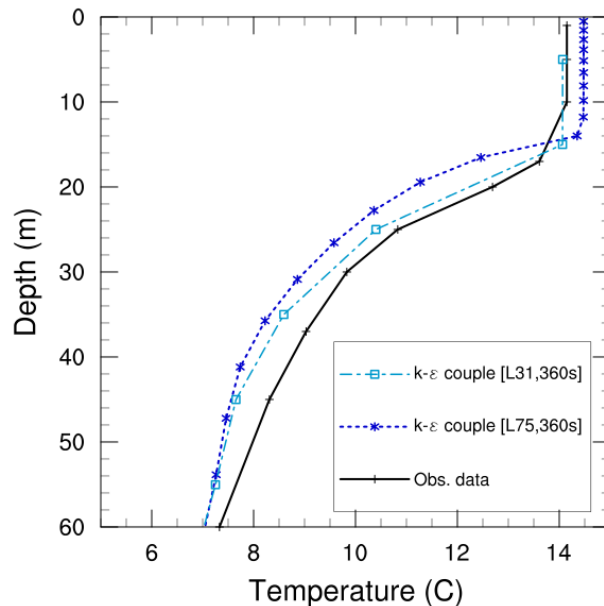


Figure 11. Daily vertical profiles of temperature for 20 August 2010: observed (black), simulated with k - ε closure, a time step of 3600 s, L31 (light blue) and L75 (dark blue). The levels of observations and configurations are marked with squares (L31) or stars (L75).